

Kinematic Bilateral Teleoperation of Wheeled Mobile Robots Subject to Longitudinal Slippage

Weihua Li, Liang Ding, Haibo Gao and Mahdi Tavakoli, *Member, IEEE*

Abstract—With the widespread use of wheeled mobile robots (WMR) in various applications, new challenges have arisen in terms of designing its control system. One of such challenges is caused by wheel slippage. This paper proposes a new method for haptic teleoperation control of a WMR with longitudinal slippage (not including sliding). In this teleoperation system, the mobile robot's linear velocity follows the master haptic interface's position. The proposed teleoperation controller also includes an acceleration-level control law for the mobile robot such that the velocity loss caused by slippage is compensated for. Information about the magnitude and timing of slippage is displayed to the human operator through haptic (force) feedback. Despite the functional benefits of displaying slippage information as haptic feedback to the user, there are system stability related concerns that have been addressed using the proposed controller. Experiments of the proposed controller demonstrate that it results in stable bilateral teleoperation with a satisfactory tracking performance.

Index Terms—Wheeled mobile robot, teleoperation, kinematics, longitudinal slippage, absolute stability.

NOMENCLATURE

r	Wheel's radius
ω, ω_d	Wheel's angular velocity and desired angular velocity
$\dot{\omega}, \dot{\omega}_d$	Wheel's angular acceleration and desired angular acceleration
a, a_d	Wheel's linear acceleration and desired linear acceleration
v, v_d	Wheel's linear velocity and desired linear velocity
S	Wheel's slippage
δ	Wheel's velocity loss caused by slippage
ε_e	Shortage of passivity for environment termination
τ_h, δ_e	Human and environment interaction forces

I. INTRODUCTION

When a wheeled mobile robot (WMR) is traveling on a slippery surface, the ideal assumption of pure rolling is not held any more, which will introduce problems for its control. With the increase in interest in planetary exploration or disaster zone exploration by WMR, researchers have started to pay more attention to the slippage phenomenon, which causes a velocity loss for the WMR relative to a desired input velocity signal [1-5]. With the introduction of

W. Li, L. Ding and H. Gao are with the State Key Laboratory of Robotics and System, Harbin Institute of Technology, Harbin, 150001 China. W. Li is also a visiting PhD student with the Department of Electrical & Computer Engineering, University of Alberta. (e-mails: liweihua.08301@gmail.com, {liangding, gaohaibo}@hit.edu.cn).

M. Tavakoli (Principal Investigator) is with the Department of Electrical & Computer Engineering, University of Alberta, Edmonton, Alberta, T6G 2V4 Canada (e-mail: mahdi.tavakoli@ualberta.ca).

the slippage, the WMR's kinematic and dynamic models are affected, creating new challenges for control. To compensate for the influence of the wheel's slippage on WMR's velocity, a few controllers for path-planning and tracking are proposed in [2-4]. A new control algorithm is proposed in [5] where the forces between the WMR and the terrain are modeled based on the value of slippage, but this slippage-dependent interaction force model is always experimental and its fidelity is limited by the uncertainty in determining its parameters [1].

Over the past decades years, significant research has been done on teleoperation systems. For a bilateral teleoperation system, the main goals are twofold: stability and transparency [6]. To meet them, many control architectures have been adopted. To ensure the teleoperation system stability, the passivity-based approaches have been widely developed and many methods have been proposed including scattering approach [7], wave variables [8], damping-injection control [9], etc. By considering velocities and forces in a teleoperation system as currents and voltages, the electromechanical system mediating between the human operator and the environment can be modeled as a two port network [10]. The necessary and sufficient conditions for absolute stability (stability under all passive terminations) of a two-port network are given by the Llewellyn's criterion [11], which is used in this paper.

Teleoperation of WMR is a natural requirement of using the robot in outer space, where appropriately providing haptic feedback (bilateral teleoperation) can enhance task performance. For bilateral teleoperation of WMR, there are two kinematics-related challenges not often experienced during teleoperation of non-mobile robots [12]: 1) the workspace of the master robot is limited but that of the slave WMR is often not or is much bigger, and 2) the wheeled mobile robot is under non-holonomic constraints so that the directions of permissible motions are restricted. Owing to WMR's unlimited workspace, the coordination of master's position (q_m) and slave's velocity (v_s) is commonly considered [12-16]. Additionally, to teleoperate the WMR in the Cartesian coordinates despite the non-holonomic constraints, a semi-autonomous control strategy is proposed in [10] by employing idempotent and generalized pseudo-inverse matrices to augment operator control with some level of assistance/autonomy. Generally, these researches are based on the ideal assumption of pure rolling (zero slippage), which is not held for slippery surfaces. We will consider the problem of *workspace mismatch* and *surface slippage* at the same time for a two-wheeled actuated mobile robot that travels forward or backward but does not rotate and, therefore, is free from non-holonomic constraints.

Therefore, while there exists work on WMR teleoperation, the wheel's slippage is rarely considered. Typically, the WMR's embedded controller is at the kinematic level and for wheel angular velocity control (the controller ensures tracking a desired angular velocity for the wheel) rather than at the dynamic level and for wheel torque control. Using kinematic control for a WMR with longitudinal slippage will inevitably result in errors between the desired and actual linear velocities for the WMR. To compensate for the velocity error caused by the slippage, we will use an acceleration-level controller for the wheel, which will be described later. Considering applications such as disaster zone exploration and motivated by understanding how the wheel's slippage influences the WMR's teleoperation, the time delay in the master-slave communication channel is not taken into account in this paper.

Kinematically, slippage is defined as a function of the wheel's angular velocity and the WMR's linear velocity [5]. The magnitude of slippage is decided by the parameters of terrain (e.g., loose soil). In the context of teleoperation of a WMR, slippage can be modeled as the *environment termination (ET)* for the slave (WMR) robot. Interestingly, as we will see later, slippage fluctuations may cause the ET to exhibit non-passive behavior, complicating the teleoperation control of the WMR. In [17], Jazayeri and Tavakoli considered the termination's non-passivity and modified the Llewellyn's absolute stability criterion through Mobius transformations. While [17] was focused on stability analysis and did not directly address controller design, in this paper we model the ET as an input non-passive system and propose compensation for its shortage of passivity, which is induced by the slippage. Also, in [17] the model of the ET was LTI (linear time invariant) while in this paper the slippage model is time-varying.

The rest of this paper is organized as follows: In Sec. II, the WMR's kinematic model with longitudinal slippage is developed, and the extent of non-passivity induced by slippage is found. In Sec. III, a stabilizing controller for bilateral teleoperation of the WMR is designed based on the modified Llewellyn's Criterion for input non-passive (INP) terminations with some level of shortage of passivity (SOP). In Sec. IV, experiments of the proposed controller are done to demonstrate the system stability. Sec. V presents the concluding remarks and future work.

II. WMR'S KINEMATIC MODEL SUBJECT TO SLIPPAGE

In this paper, a two-wheel actuated mobile robot is considered as Fig. 1(a) shows. The two back wheels are the driving wheels separately controlled by two motors and the front wheel is free of actuation and steering and driven by the two back wheels. It is assumed that the WMR only travels forward or backward but does not rotate and, therefore, is free from non-holonomic constraints.

For such a mobile robot, in the ideal case of pure rolling, its linear velocity v will be equal to its angular velocity ω multiplied by each wheel's radius r . From the control perspective, as seen in Fig. 1(b), an angular velocity-level controller is embedded in the WMR. We will assume that, in Fig. 1(b), the transfer function from ω_d to ω is unity. Therefore, the WMR's kinematic model incorporating the angular velocity controller can be expressed as

$$v = v_d, \quad (1)$$

where $v_d = r\omega_d$.

When the WMR is traveling on a soft terrain (e.g., loose soil or sand), due to the limited friction force generated by the terrain and possible opposing external forces such as that coming from hitting an obstacle, the wheel's linear velocity v will not be equal to the wheel's angular velocity ω times the wheel's radius r . In fact, the phenomenon of longitudinal slippage will occur on the contact surface between the wheel and the terrain. Slippage S can be defined as [5]

$$S = \begin{cases} (r\omega - v)/v & (\omega \neq 0) \\ 0 & (\omega = 0) \end{cases}. \quad (2)$$

The above relationship between the wheel's linear velocity v and angular velocity ω can be modeled by the feedback loop in Fig. 1(b).

In the ideal case that the transfer function of the angular velocity-level controller is 1 (i.e., $\omega_d = \omega$), we have $r\omega = v_d$. In this case, (2) can be written as $S = (v_d - v)/v$. Let us define δ as

$$\delta = v_d - v, \quad (3)$$

where δ is the velocity loss caused by slippage. It is immediate based on (2) that $\delta = Sv$.

Evidently, with the influence of slippage, the embedded angular velocity controller cannot result in good linear velocity tracking any more. Therefore, we consider using an *embedded angular acceleration-level* controller that works based on the difference of the desired velocity and the actual velocity as shown in Fig. 1(c). We will assume that the transfer function from $\dot{\omega}_d$ to $\dot{\omega}$ is unity. While the angular acceleration-level controller in Fig. 1(c) has a model quite similar to the angular velocity-level controller in Fig. 1(b), the WMR model relating the wheel's angular acceleration and the WMR's linear acceleration is harder to obtain in the presence of slippage. However, by differentiating $Sv = r\omega - v$ obtained from (2) we can get

$$r \left(\dot{\omega} - \underbrace{\frac{1}{r}(S\dot{v} + \dot{S}v)}_{\text{slippage model}} \right) = \dot{v}. \quad (4)$$

It should be noted that S and \dot{S} are both time-varying functions, thus necessitating the time-domain expression of the model.

In Fig. 1(c), a_d is a desired linear acceleration for the WMR determined based on the linear velocity error, which is then passed to the angular acceleration-level controller embedded in the WMR. Since we have assumed that, in Fig. 1(c), the transfer function from $\dot{\omega}_d$ to $\dot{\omega}$ is unity, Fig. 1(c) can be simplified as Fig. 1(d).

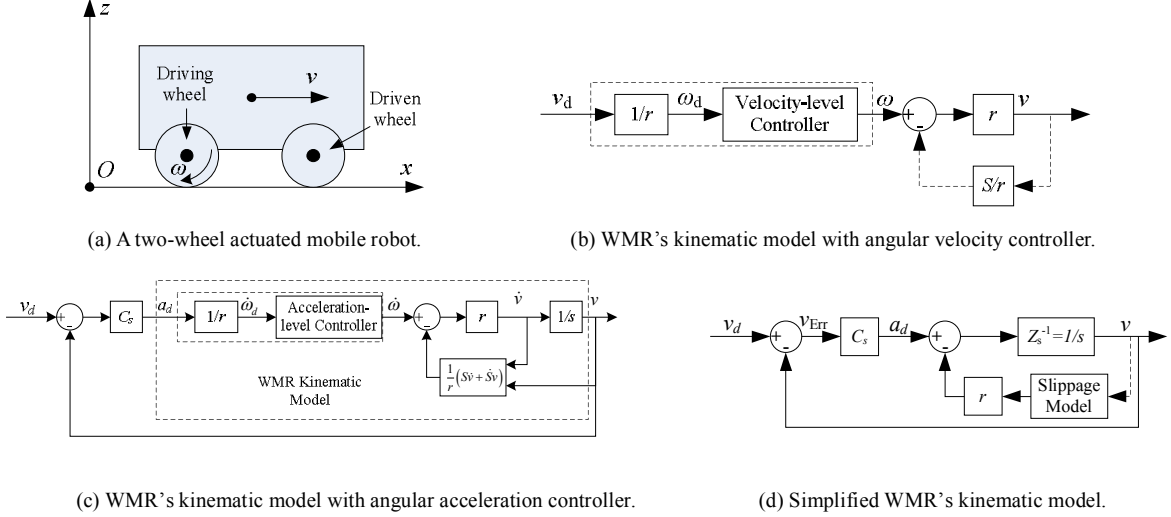


Figure 1. WMR's kinematic model and control.

III. TELEOPERATION OF A WMR

A. Slave Robot's Model

In this section, we will consider the model of a WMR when it acts as the slave robot of a teleoperation system. We are interested in modeling the terrain-dependent longitudinal slippage as the “environment” with which the slave robot interacts. From (3) and the equation $\delta = Sv$, we can get

$$\dot{\delta}(t) = S(t)\dot{v}(t) + \dot{S}(t)v(t). \quad (5)$$

From the definition of the slippage (2), it appears to be a function of the WMR's linear velocity and its wheel angular velocity. However, the slippage actually is not decided by these, but by the WMR/terrain contact characteristics. Therefore, $\dot{\delta}(t)$ in (5) can be seen as the contribution of the external environment (terrain) to deciding the WMR's linear acceleration where there is longitudinal slippage.

In this paper, we consider the case of $r\omega > v$, that is $S > 0$, corresponding to the case where the wheel slippage causes a reduction in the linear velocity of the WMR – we do not consider the case of *wheel sliding* that would result in the linear velocity being increased. We here assume that the rate of change of slippage is constrained by $\dot{S}_L < \dot{S} < \dot{S}_U$ where \dot{S}_L and \dot{S}_U are actually decided by the WMR's states and terrain's parameters.

Defining the control input $u_s = a_d$ and the environment interaction force δ_e , the kinematic model of the slave robot can be found based on (4) and (5) as

$$\dot{v}_s = u_s - \delta_e, \quad (6)$$

where $\delta_e(t) = S(t)\dot{v}_s(t) + \dot{S}(t)v_s(t)$.

The above equation provides a straightforward model of the WMR as the slave robot in interaction with an environment. Please note that the environment interaction force δ_e provides a generalization of the terrain-dependent slippage-induced force. The following property is proposed to determine the passivity or non-passivity of the system described by (5).

Property 1 The LTV system (5), when \dot{S} is negative, is input non-passive (INP) with a shortage of passivity (SOP) of $-0.5\dot{S}_L$.

Proof: With the input $v_s(t)$ and output $\delta_e(t)$, the system (5) satisfies the following inequality for all $v_s(t)$ and $T \geq 0$:

$$\begin{aligned}
\int_0^T \delta_e(t)v_s(t)dt &= \int_0^T v_s(t)(S(t)\dot{v}_s(t) + \dot{S}(t)v_s(t))dt \\
&= \underbrace{V(T) - V(0)}_{Z_{e1}} + \underbrace{\frac{1}{2} \int_0^T \dot{S}(t)v_s(t)v_s(t)dt}_{Z_{e2}} \\
&\geq -V(0) + \underbrace{\frac{1}{2} \int_0^T \dot{S}(t)v_s(t)v_s(t)dt}_{Z_{e2}}, \tag{7} \\
&\geq -V(0) + \frac{1}{2} \underbrace{\min(\dot{S}(t)) \int_0^T v_s(t)v_s(t)dt}_{Z_{e2}} \\
&\geq -V(0) + \frac{1}{2} \underbrace{\dot{S}_L \int_0^T v_s(t)v_s(t)dt}_{Z_{e2}}
\end{aligned}$$

where $V(t) = \frac{1}{2}S(t)v_s^2(t) \geq 0$ since $S(t) \geq 0$. As shown above, the input-output passivity integral [18] has been decomposed into two parts: an always passive part (Z_{e1}) and a potentially active part (Z_{e2}). When Z_{e2} is positive, this system will dissipate energy and cause an excess of passivity, so this system is strictly passive. However, when Z_{e2} is negative, this system may accumulate energy and become INP with the largest (worst-case) SOP of $-0.5\dot{S}_L$. In short, (7) shows the ET can be an INP system with a SOP of $-0.5\dot{S}_L$.

B. Master robot's model

For a single-joint master robot, the dynamics can be written as

$$M_m\ddot{q}_m + B_m\dot{q}_m = \tau_m + \tau_h, \tag{8}$$

where M_m and B_m are the robot's mass and damping coefficients, q_m is the degree of freedom, τ_m and τ_h are the forces/torques applied by the motor and human.

In general non-mobile robot teleoperation applications, the master and slave velocities (and positions) are synchronized. However, owing to the unlimited workspace of the WMR, the coordination between the master's position q_m and the slave's velocity v_s needs to be adopted here. Inspired by [12], a new variable $r_m = \lambda\dot{q}_m + q_m$ where $0 < \lambda < 1$ is employed to be used instead of \dot{q}_m in the impedance matrix; in this way, the problem will become of one coordinate of r_m and v_s . When λ and/or \dot{q}_m are small, an approximate coordination of position-velocity ($q_m \approx v_s$) is achieved between the master robot and the slave mobile robot.

This change of variable also necessitates defining a new control signal. The controller τ_m in (8) is designed as $\tau_m = \tau_m^* + \bar{\tau}_m$ consisting of a local controller τ_m^* and $\bar{\tau}_m$ that will be designed in Sec. IV. In terms of the new variable r_m and with the local controller $\tau_m^* = -B_{Lv}\dot{q}_m - B_{Lp}q_m$, the master robot's dynamic model (8) can be rewritten as

$$\bar{M}_m \dot{r}_m + \bar{B}_m r_m = \bar{\tau}_m + \tau_h, \quad (9)$$

where $\bar{M}_m = M_m/\lambda$, $\bar{B}_m = B_{Lp}$ and $B_{Lv} = \frac{M_m}{\lambda} + \lambda B_{Lp} - B_m$. Then, the master robot's impedance model will become:

$$Z_m = \frac{\mathcal{L}(\bar{\tau}_m + \tau_h)}{\mathcal{L}(r_m)} = \bar{M}_m s + \bar{B}_m.$$

In addition, the human operator model should be written in terms of the new variable r_m as $\tau_h = \bar{Z}_h r_m$. However, as [12] presented, we assume the human operator can adjust his/her impedance to ensure the passivity of its impedance when augmented with the position/velocity transformation. This assumption is seen in an overwhelming majority of the teleoperation literature [12, 19].

IV. MAIN RESULTS

A. Bilateral Teleoperation of WMR

Following the above-described decomposition of the ET, the WMR teleoperation system can be modeled as in Fig. 2. Outside the dashed box reside the passive components of the human and environment terminations. That part of the ET's impedances that resides inside the dashed box may be passive or active. The ET may show a SOP as large as ε_e (based on (7), $\varepsilon_e = -0.5\dot{S}_L$). Therefore, the Llewellyn's absolute stability criterion cannot be directly used for the Teleoperation System block in Fig. 2 as not both of its terminations are passive.

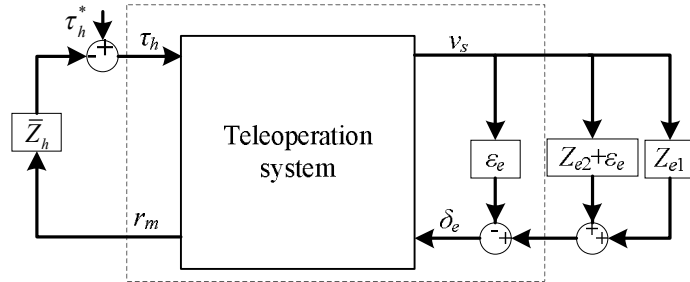


Figure 2. WMR's teleoperation system after termination's decomposition.

However, the Llewellyn's criterion can be applied to the two-port network in the dashed box in Fig. 2 because both of its terminations are passive as explained below. Recall that the environment impedance was split to an always passive part (Z_{e1}) and a potentially active part (Z_{e2}). The potential active component Z_{e2} of the ET can be decomposed into the two parts shown in Fig. 2 as $Z_{e2} = (Z_{e2} + \varepsilon_e) - \varepsilon_e$. Obviously, $(Z_{e2} + \varepsilon_e)$ is passive because ε_e is the worst-case SOP of the ET. As a result, the modified ET is always passive, and the active component ($-\varepsilon_e$) is included in the teleoperation system's model. For the teleoperation system with the master robot (9) and the slave robot (6), the impedance matrix model for the two-port network in the dashed box in Fig. 2 is

$$\begin{bmatrix} \tau_h \\ \delta_e + \varepsilon_e v_s \end{bmatrix} = \begin{bmatrix} Z_{11} & Z_{12} \\ Z_{21} & Z_{22} \end{bmatrix} \begin{bmatrix} r_m \\ -v_s \end{bmatrix}. \quad (10)$$

Lemma 1 (Llewellyn's criterion [11]) The two-port network (10) is absolutely stable (i.e., the overall system in Fig. 2 is bounded-input/bounded-output stable assuming the passivity of both terminations) if and only if

- (1) $Z_{11}(s)$ and $Z_{22}(s)$ have no poles in the right half plane;
- (2) Any poles of $Z_{11}(s)$ and $Z_{22}(s)$ on the imaginary axis are simple with real and positive residues;
- (3) For $s = j\omega$ and all real values of ω :

$$\begin{aligned} \operatorname{Re}(Z_{11}) &\geq 0 \\ \operatorname{Re}(Z_{22}) &\geq 0 \\ 2\operatorname{Re}(Z_{11})\operatorname{Re}(Z_{22}) - \operatorname{Re}(Z_{12}Z_{21}) - |Z_{12}Z_{21}| &\geq 0 \end{aligned} \quad (11)$$

B. Teleoperation System Design

To achieve a stable teleoperation system with good performance, various teleoperation control architectures exist. Four-channel (4CH) bilateral teleoperation of the WMR, as shown in Fig. 3(a), can represent the other structures through the appreciate selection of C_1 to C_6 [19].

In this paper, we consider two bilateral teleoperation control architectures: The direct force reflection (DFR) of the environment force including the slippage-induced force (5), and the position error based (PEB) control where the force feedback is proportional to the difference of the slave's desired velocity and its actual velocity [19]. Lemma 1 will be employed to find the stability conditions in the presence of these two controllers.

1) PEB architecture

The PEB teleoperation scheme of WMR is shown in Fig. 3(b). The PEB control laws are

$$\begin{cases} u_s = C_s (r_m - v_s) + K_s v_s \\ \bar{\tau}_m = -C_m (r_m - v_s) \end{cases} \quad (12)$$

Note that while $u = u_s - \delta_e$, and $\tau = \bar{\tau}_m + \tau_h$ are applied to the slave and master, respectively, the controllers outputs are u_s and $\bar{\tau}_m$. Then, the impedance matrix in (10) is found to be

$$Z = \begin{bmatrix} \bar{M}_m s + \bar{B}_m + C_m & C_m \\ C_s & s + C_s + K_s - \varepsilon_e \end{bmatrix}. \quad (13)$$

Using Lemma 1, the PEB controller should meet the following conditions for stability of the teleoperation system:

$$\begin{aligned} \bar{B}_m + C_m &\geq 0 \\ C_s + K_s - \varepsilon_e &\geq 0 \\ 2(\bar{B}_m + C_m)(C_s + K_s - \varepsilon_e) - \operatorname{Re}(C_s C_m) - |C_s C_m| &\geq 0 \end{aligned} \quad (14)$$

The solution of (14) is

$$\begin{aligned} C_m, C_s &\geq 0 \\ \bar{B}_m &\geq 0 \\ K_s &\geq \varepsilon_e \end{aligned} \quad (15)$$

2) DFR architecture

The DFR teleoperation architecture is shown in the block diagram of Fig. 3(c). The DFR controller is designed as

$$\begin{cases} u_s = C_s (r_m - v_s) + K_s v_s \\ \bar{\tau}_m = -\delta_e \end{cases} \quad (16)$$

Then, the impedance matrix in (10) is found as

$$Z = \begin{bmatrix} \bar{M}_m s + \bar{B}_m + C_s & s + C_s + K_s - \varepsilon_e \\ C_s & s + C_s + K_s - \varepsilon_e \end{bmatrix} \quad (17)$$

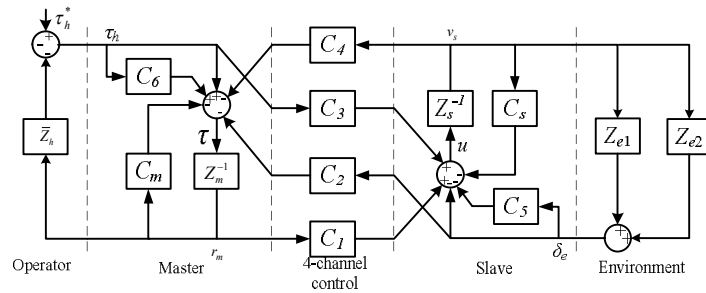
In order to maintain the entire teleoperation system stable, according to Lemma 1, the following conditions should be met:

$$\begin{aligned} \bar{B}_m + C_s &\geq 0 \\ C_s + K_s - \varepsilon_e &\geq 0 \\ 2(C_s + \bar{B}_m)(C_s + K_s - \varepsilon_e) - \\ \operatorname{Re}(C_s(C_s + K_s - \varepsilon_e)) - |C_s(C_s + K_s - \varepsilon_e) + C_s \omega j| &\geq 0 \end{aligned} \quad (18)$$

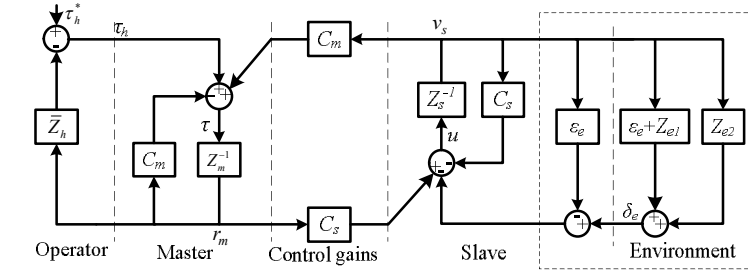
Simplification of (18) results in the following conditions

$$\begin{aligned} C_s &\geq 0 \\ \bar{B}_m &\geq 0 \\ K_s &\geq \varepsilon_e \quad (C_s \gg \omega) \end{aligned} \quad (19)$$

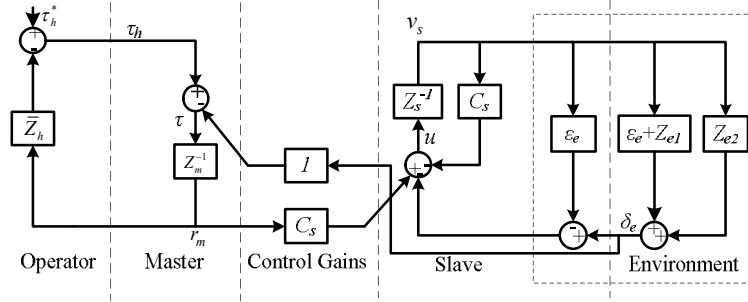
Conditions (15) and (19) give the absolutely stability conditions for the WMR's bilateral teleoperation system. Note that in (15) and (19), the maximum SOP of the environment is used. This means that if the SOP value is less, we may have stability even when (15) and (19) calculated for the worst-case SOP is violated. In addition, since the non-passivity of the ET is compensated for by K_s at the slave robot, the parameters of C_m and \bar{B}_m are affected by the chosen master robot.



(a) 4-channel teleoperation control of WMR.



(b) PEB teleoperation control of WMR.



(c) DFR teleoperation control of WMR.

Figure 3. Bilateral teleoperation control of WMR.

V. CASE STUDIES

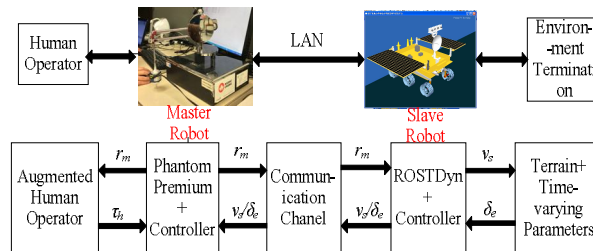
In the case studies below, we consider the teleoperation of a mobile robot in an environment with slippage. The slippage varies with soil's mechanical parameters (e.g., friction angle) [20] and the terrain's parameters (e.g., slope angle). Limited by implementation issues concerning recreating specific terrain characteristics that give rise to certain shortage of passivity of the environment model, we perform semi-physical experiments to validate the proposed PEB and DFR teleoperation of the WMR under longitudinal slippage.

A. Experimental setup

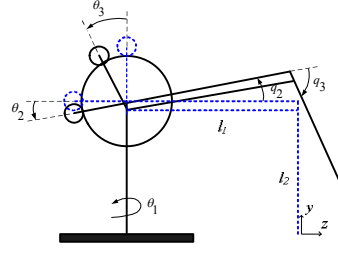
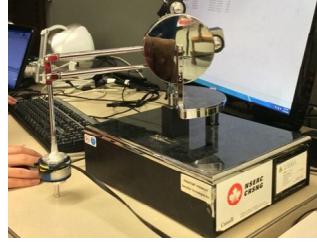
To validate the proposed methods, experiments are done using a Phantom Premium 1.5A haptic device (master robot) and ROSTDyn (slave robot). The experimental system is detailed below.

(1) Master robot and human operator

As shown in Fig. 4(a), in our WMR's bilateral teleoperation system, the master robot is a Phantom Premium 1.5A haptic device (Geomagic Inc., Wilmington, MA, USA) (Fig. 4(b)), and the slave robot (WMR) is a WMR's simulation platform called ROSTDyn which has been developed by the authors [21], and the communication between the master robot and the slave robot is implemented using local area network (LAN). Considering just one degree of freedom (DOF) motion, the first joint q_1 of the Phantom is used and the other two joints are locked by a high gain position controller ($q_2=q_3=0$). Based on the research results from [22], the Phantom's inertia is $M_m=0.0035$. In (9), $\lambda=0.1$ and $B_{Lv}=-0.035$.



(a) Scheme of WMR bilateral teleoperation system.



(b) The master Phantom 1.5A robot.

Figure 4. Experiment platform setup of WMR bilateral teleoperation system.

In the experiments, based on (9), the force applied on the master robot by human operator is estimated as

$$\tau_h = \bar{M}_m \dot{r}_m + \bar{B}_m r_m - \bar{\tau}_m. \quad (20)$$

(2) Slave robot and environment

As shown in Fig. 4(a), ROSTDyn is used as the slave robot and developed based on Vortex software (CMLabs, Montreal, Canada) and the simplified terramechanics model. ROSTDyn can perform a real-time simulation with a good fidelity [21]. In this paper, we use ROSTDyn to simulate a WMR moving on a soft terrain, which causes slippage. The following is the terramechanics model between the wheel and terrain in ROSTDyn:

$$\begin{cases} F_N = rb\sigma_m A + rb\tau_m B = AX + BY \\ F_{DP} = rb\tau_m A - rb\sigma_m B = AY - BX, \\ M_R = r^2 b(\theta_1 - \theta_2)\tau_m / 2 = rCY \end{cases} \quad (21)$$

$$\text{where } A = \frac{\cos\theta_m - \cos\theta_2}{\theta_m - \theta_2} + \frac{\cos\theta_m - \cos\theta_1}{\theta_1 - \theta_m};$$

$$B = \frac{\sin\theta_m - \sin\theta_2}{\theta_m - \theta_2} + \frac{\sin\theta_m - \sin\theta_1}{\theta_1 - \theta_m}; \quad C = (\theta_1 - \theta_2) / 2;$$

$$X = rb\sigma_m; \quad Y = rb\tau_m;$$

$$\tau_m = E(c + \sigma_m \tan\varphi); \quad \sigma_m = K_s r^N (\cos\theta_m - \cos\theta_1)^N;$$

$$E = 1 - \exp\{-r[(\theta_1 - \theta_m) - (1-s)(\sin\theta_1 - \sin\theta_m)] / K\}; \quad K_s = K_c / b + K_\varphi; \quad N = n_0 + n_1 s.$$

In (21), F_N is the normal force, F_{DP} is the drawbar pull force, and M_R is the moment generated by the interaction between the wheel and the terrain, s is the slippage of a wheel and φ is the internal friction angle. The other parameters are defined in [20].

The terrain has a slope with an angle of 15° , and its size is $10\text{m} (x) \times 10\text{m} (y)$. Since we are focusing on creating a nonpassive ET caused by the slippage, and the slippage model cannot be directly given, the most sensitive parameter to the slippage [23], which is φ in (21), is considered and set as a terrain-varying function. In practice, φ is decided by the soil's characteristics. The following model makes the terrain become harder as the WMR travels forward:

$$\varphi = \begin{cases} 1.25 & (6.1 \leq x < 10) \\ 0.5 + 0.25(x - 3.1) & (3.1 \leq x < 6.1) \\ 0.5 & (0 < x < 3.1) \end{cases}. \quad (22)$$

Here, x is the WMR position along the moving direction. In the case of climbing a sloped terrain, the bigger

the φ , the smaller the slippage, and this will cause a negative \dot{S} while S is positive, which causes the ET's potential non-passivity. In practice, if we can obtain the mechanical characteristics of the terrain and the terrain's digital elevation model (DEM), the slippage can be roughly predicted by (21). However, a conservative \dot{S} is sometimes preferable for the WMR as its safety is superior to performance. Choosing too conservative a value for $\min(\dot{S})$ can decrease the force tracking performance and the velocity tracking performance with the designed control parameters. Before implementing the following experiments, the \dot{S} range is decided via through calculations implemented by the ROSTDyn simulation platform.

B. PEB Teleoperation Experiments

In the experiments involving WMR bilateral teleoperation with PEB architecture, to validate the proposed methods based on (15), the parameters are set to be

Case I: $C_m = 15, C_s = 8, K_s = 0$;

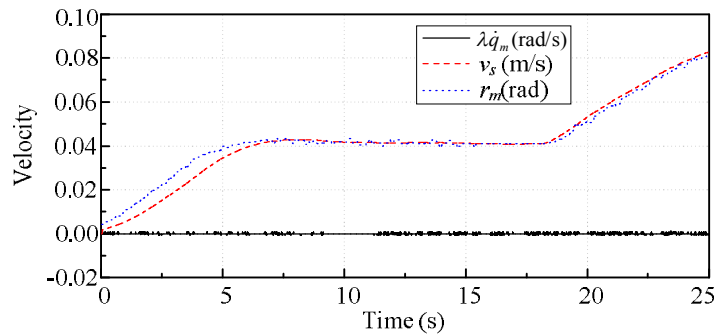
Case II: $C_m = 15, C_s = 8, K_s = 0.8$.

Case I ignores the ET's shortage of passivity, but the controller's parameters meet the Llewellyn's criterion while $\varepsilon_e = 0$. Case II also considers the ET's shortage of passivity. The experimental results are shown in Fig. 5 (Case I) and Fig. 6 (Case II).

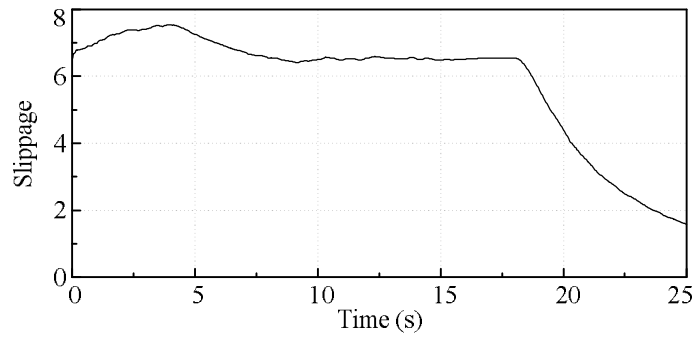
For the PEB architecture, the master robot provides r_m , which acts as a reference value for to the slave robot's velocity. Owing to the time-varying slippage, the actual slave robot's velocity v_s may be different from this commanded velocity and a velocity-error is caused, which is fed back to the master robot as a force. If r_m is bigger than v_s , a backward force will be felt by the human operator that pushes back on the master robot; if r_m is smaller than v_s , a forward force will be felt by the human operator that pulls the master robot forward. Therefore, in PEB teleoperation, force feedback guides the human operator to give a more effective command to the slave WMR.

The position-velocity plots of the experiments in Case I (Fig. 5(a)) show that the PEB system with nonpassive ET is unstable. The ET's non-passivity (Fig. 5(c)), which is caused by the WMR's slippage (Fig. 5(b)), will inject energy to the slave robot and make the actual velocity v_s increase. As a result, the position-velocity coordination is not maintained and the human operator cannot control the slave WMR.

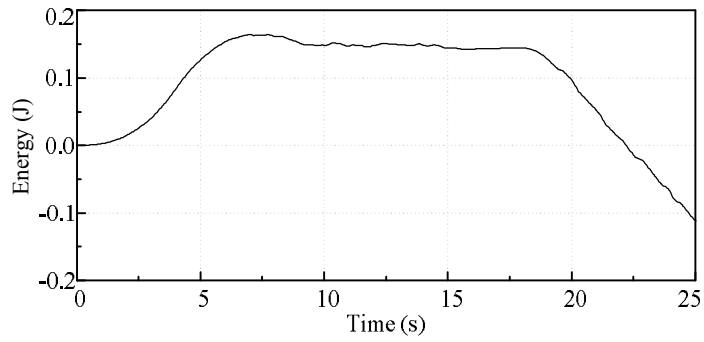
With Case II, on the other hand, the termination's non-passivity is completely compensated for with the modified ET (Fig. 6(c)), resulting in a stable system (Fig. 6(a)). Note that it was reasonable to set K_s (and ε_e) at 0.8 based on Fig. 6(b) and calculation of $\varepsilon_e = -0.5\dot{S}_L$, in which the slope of the steepest decrease in the slippage is used. The position-velocity coordination is maintained well (Fig. 6(a)), meaning that the human can control the WMR's velocity at a desired level. Also, it is easy for the human operator to feel the velocity error influenced by the terrain/WMR slippage (Fig. 6(d)). Note that in PEB teleoperation, the ratio of human/master contact force to the slave/environment contact force is equal to the ratio of the master controller gain to the slave controller gain. Thus, in our experiments, the ratio of forces seen in Fig. 6(d) is resulted.



(a) Position-velocity coordination.

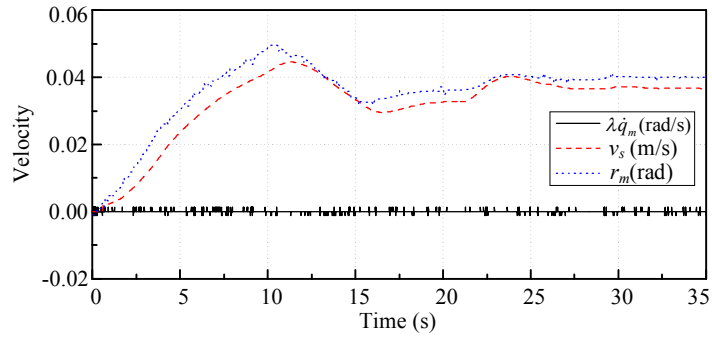


(b) Terrain/WMR slippage.

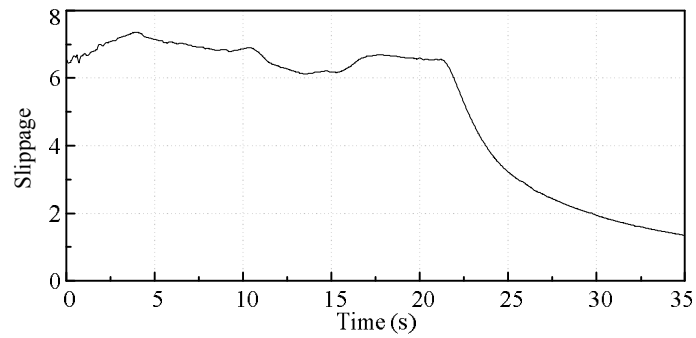


(c) Energy generated by ET.

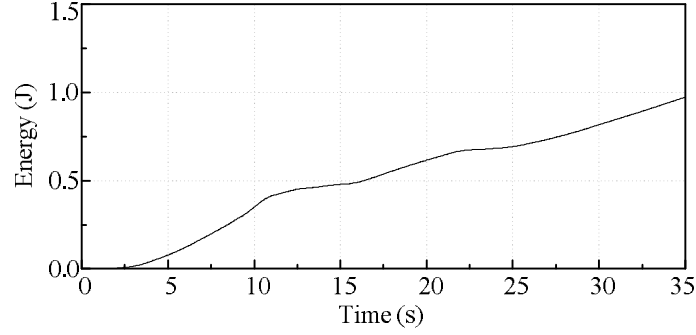
Figure 5. Experimental results for PEB in Case I.



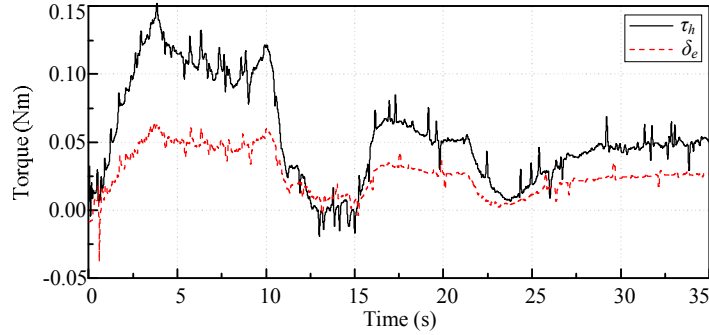
(a) Position-velocity coordination.



(b) Terrain/WMR slippage.



(c) Energy generated by modified ET.



(d) Force tracking performance (τ_h and δ_e).

Figure 6. Experimental results for PEB with Case II.

C. DFR Teleoperation Experiments

In the experiments involving WMR bilateral teleoperation with DFR architecture, to validate the proposed methods based on (19), the teleoperator parameters are set to be:

Case I: $C_s = 20$, $K_s = 0$;

Case II: $C_s = 20$, $K_s = 0.8$.

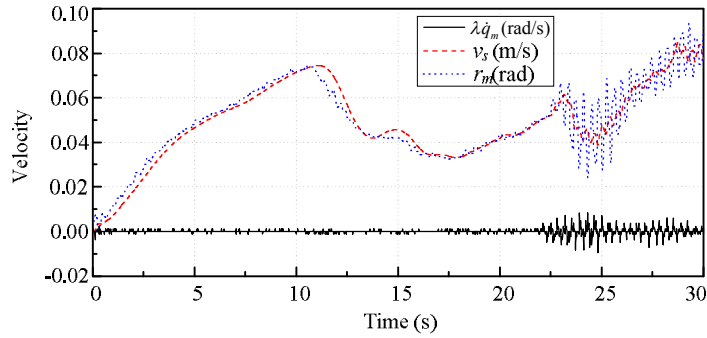
Case I ignores the ET's shortage of passivity, but the controller's parameters meet the Llewellyn's criterion while $\varepsilon_e = 0$. Case II also considers the ET's shortage of passivity. The experimental results are shown in Fig. 7 (Case I) and Fig. 8 (Case II). Note that here the force feedback is the modified environment force (seeing Fig. 3(c)). The terrain parameters and φ are same as in the case of PEB.

In the DFR architecture, similar to PEB, the master robot provides r_m , which acts as a reference value for the slave robot's velocity. Unlike PEB which fed back the *velocity error* as a force to the human operator, in DFR the ET's force δ_e is fed back to the human operator, which can be seen as an *acceleration error* based on (4). Physically speaking, if δ_e is positive, which means that the actual acceleration of the slave robot is smaller than the commanded acceleration, a backward force will be felt by the human operator informing the user about this deficiency in the WMR's acceleration. If δ_e is negative, which means that the actual acceleration of the slave robot is bigger than the commanded acceleration, a forward force will be felt by the human operator to signal an excess in the WMR's acceleration. In both the PEB and the DFR force feedback schemes, the human operator receives useful feedback from the environment of the slave robot that should pave the ground for a more effective command; one feedback is about velocity error and the other is about acceleration error.

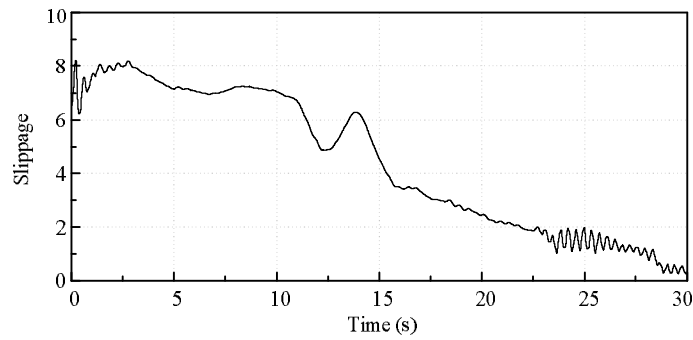
The position-velocity plots of the experiments in Case I (Fig. 7(a)) show that the DFR system with nonpassive ET is unstable. The ET's non-passivity (Fig. 7(c)), which is caused by the WMR's slippage (Fig. 7(b)), will inject energy to the slave robot and make the actual velocity v_s oscillate. As a result, the

position-velocity coordination is not maintained and the human operator (Fig. 7(d)) cannot control the slave WMR. In this experiment, owing to the big oscillation of the master robot's position, the coordination between q_m and v_s is poor as \dot{q}_m is big (Fig. 7(a)).

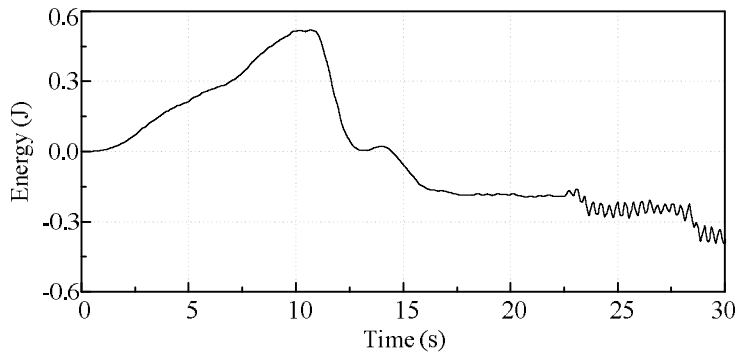
With Case II, on the other hand, the termination's non-passivity is completely compensated for with the modified ET (Fig. 8(c)), resulting in a stable system (Fig. 8(a)). Similarly, here it was reasonable to set K_s (and ε_e) at 0.8 based on Fig. 8(b) and calculation of $\varepsilon_e = -0.5\dot{S}_L$. The position-velocity coordination is maintained well (Fig. 8(a)), meaning that the human can control the WMR's velocity at a desired level. Also, it is easy for the human operator to feel the terrain/WMR interaction force (Fig. 8(d)).



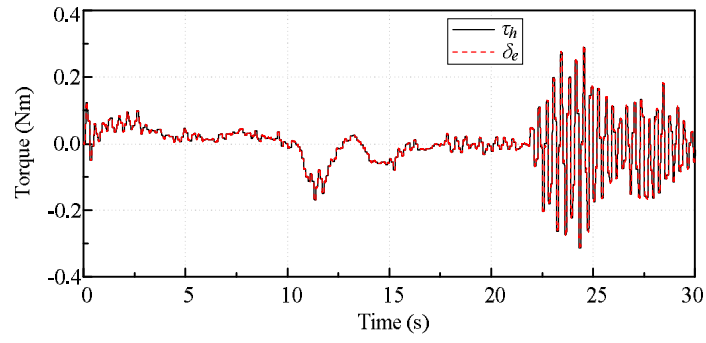
(a) Position-velocity coordination.



(b) Terrain/WMR slippage.

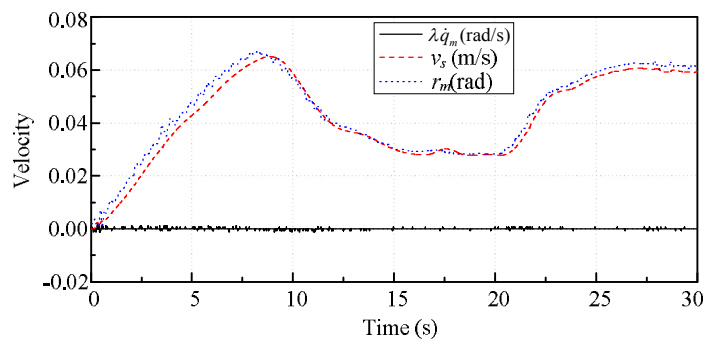


(c) Energy generated by ET.

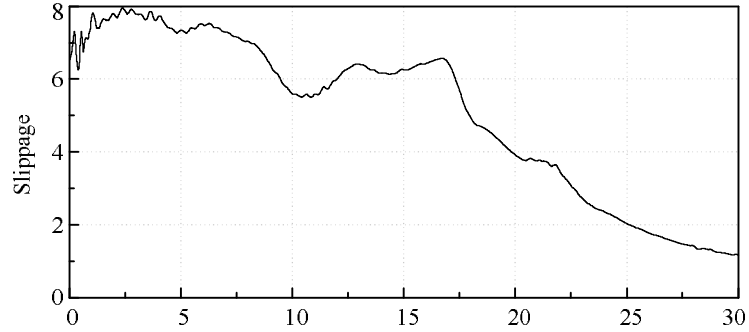


(d) Force tracking performance (τ_h and δ_e).

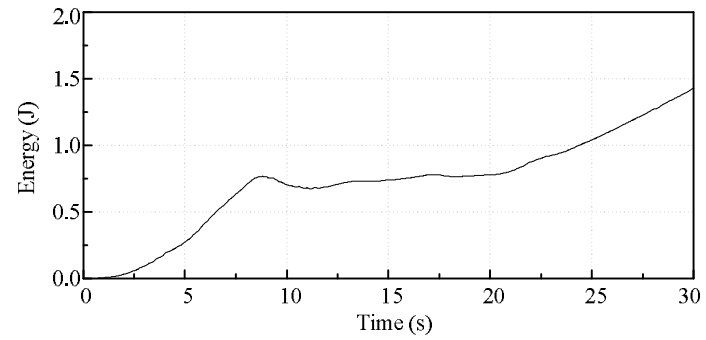
Figure 7. Experimental results for DFR with Case I.



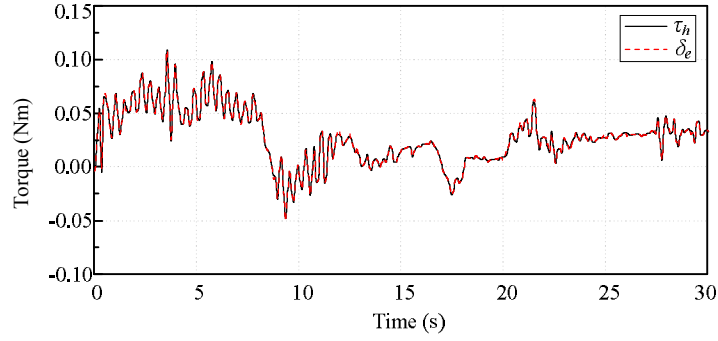
(a) Position-velocity coordination.



(b) Terrain/WMR slippage.



(c) Energy generated by modified ET.



(d) Force tracking performance (τ_h and δ_e).

Figure 8. Experimental results for DFR with Case II.

In addition to these typical experiments, many different sets of controller parameters and terrain parameters were also tested to optimize the velocity tracking performance and the force tracking performance. In all experiments, the stability conditions were satisfied. It was found that under the stability conditions, the bigger the K_s is, the worse the velocity tracking performance of the slave robot and the force tracking performance of the human operator are. It was also found that increasing the C_s value can increase the velocity tracking performance of the slave robot to some extent while increasing C_m can increase the ratio of the force felt by the human operator.

In summary, from the experimental results, it is concluded that the ET's SOP may result in an unstable system even if the controller parameters meet the Llewellyn's criterion. The proposed method, which is a variant of the Llewellyn's criterion through decomposing the nonpassive ET and including the potentially active component in the WMR's teleoperation system, can effectively lead to a stable system.

VI. CONCLUSION

A new method for haptic teleoperation control of a WMR with longitudinal slippage is proposed in this paper. In this teleoperation system, the mobile robot's linear velocity follows the master haptic interface's position. We propose a teleoperation controller including an acceleration-level control law for the mobile robot such that the velocity loss caused by slippage is compensated for. Another contribution of the paper lies in showing the non-passivity of the teleoperation system's environment termination caused by the WMR's slippage. The paper then provides a stability analysis of the teleoperation system through decomposing the non-passivity into a passive component and an active component. Stabilizing teleoperation controllers can then be designed as shown in the paper. Experiments of the proposed controllers demonstrate the validity of the theoretical findings. In the future, the WMR's rotation motion and teleoperation time delays will be considered in the stability analysis and control design.

REFERENCE

- [1] L. Ding, K. Nagatani, K. Sato, et al.: 'Terramechanics-based high-fidelity dynamics simulation for wheeled mobile robot on deformable rough terrain'. Proc. IEEE Int. Conf. Robot. Autom, Anchorage, Alaska, USA, May 2010, pp. 4922-4927.
- [2] Lin S., Chang L.-H. and Yang P.-C.: 'Adaptive critic anti-slip control of wheeled autonomous robot', IET Control Theory & Applications, 2007, 1, (1), pp. 51-57.
- [3] G. Ishigami, K. Nagatani, and K. Yoshida: 'Path Following Control with Slip Compensation on Loose Soil for Exploration Rover'. Proc. IEEE/RSJ Int. Conf. Intell. Robots Syst., Beijing, China, Oct. 2006, pp. 5552-5557.
- [4] Yoo S.J.: 'Adaptive tracking control for a class of wheeled mobile robots with unknown skidding and slipping', IET Control Theory & Applications, 2010, 4, (10), pp. 2109-2119.
- [5] Yu Tian and Nilanjan Sarkar: 'Control of a Mobile Robot Subject to Wheel Slip', J. Intell. Robot Syst., 2014, 74, (4), pp. 915-929.
- [6] Peter F. Hokayem, MarkW. Spong: 'Bilateral teleoperation: An historical survey', Automatica, 2006, 42, pp. 2035-2057.
- [7] Anderson, R. J., Spong, M. W.: 'Bilateral control of teleoperators with time delay', IEEE Transactions on Automatic Control, 1989, 34, (5), pp. 494-501.
- [8] G. Niemeyer and J. E. Slotine: 'Telemanipulation with time delays', International Journal of Robotics Research, 2004, 23, (9), pp. 873-890.

- [9] Emmanuel Nuno, Romeo Ortega, Nikita Barabanov, and Luis Basanez, 'A Globally Stable PD Controller for Bilateral Teleoperators', *IEEE Transactions on Robotics*, 2008, 24, (3), pp. 753-758.
- [10] B. Hannaford: 'A design framework for teleoperators with kinesthetic feedback', *IEEE Trans. Robot. Autom.*, 1989, 5, (4), pp. 426-434.
- [11] S. Haykin: 'Active Network Theory: Reading' (Addison-Wesley, MA, USA, 1970).
- [12] Dongjun Lee, Oscar Martinez-Palafox, and Mark W. Spong: 'Bilateral Teleoperation of a Wheeled Mobile Robot over Delayed Communication Network'. *Proc. IEEE Int. Conf. Robot. Autom.*, Orlando, USA, May 2006, pp. 3298-3303.
- [13] Ildar Farkhatdinov and Jee-Hwan Ryu: 'Improving Mobile Robot Bilateral Teleoperation by Introducing Variable Force Feedback Gain'. *Proc. IEEE/RSJ Int. Conf. Intell. Robots Syst.*, Taipei, May 2010, pp. 5812-5817.
- [14] Ware J. and Pan Y.-J: 'Realisation of a bilaterally teleoperated robotic vehicle platform with passivity control', *IET Control Theory & Applications*, 2011, 5, (8), pp. 952-962.
- [15] Ha Van Quang, Ildar Farkhatdinov and Jee-Hwan Ryu: 'Passivity of Delayed Bilateral Teleoperation of Mobile Robots with Ambiguous Causalities: Time Domain Passivity Approach', *Proc. IEEE/RSJ Int. Conf. Intell. Robots Syst.*, Vilamoura, Algarve Portugal, Oct. 2012, pp. 2635-2640.
- [16] Pawel Malysz and Shahin Sirouspour: 'A Task-space Weighting Matrix Approach to Semi-autonomous Teleoperation Control'. *Proc. IEEE/RSJ Int. Conf. Intell. Robots Syst.*, San Francisco, USA, Oct. 2011, pp. 645-652.
- [17] Ali Jazayeri, Mahdi Tavakoli, 'Bilateral teleoperation system stability with non-passive and strictly passive operator or environment', *Control Engineering Practice*, 2015, 40, pp. 45-60.
- [18] R. Lozano, B. Maschke, B. Brogliato, and O. Egeland: 'Dissipative Systems Analysis and Control: Theory and Applications' (Springer-Verlag New York, Inc., Secaucus, NJ, USA, 2007).
- [19] Mahdi Tavakoli, Arash Aziminejad, Rajni V. Patel, and Mehrdad Moallem: 'High-Fidelity Bilateral Teleoperation Systems and the Effect of Multimodal Haptics', *IEEE Trans. Syst. Man Cybern.-Part B*, 2007, 37, (6), pp. 1512-1528.
- [20] Haibo Gao, Weihua Li, Liang Ding et al: 'A Method for On-line Soil Parameters Modification to Planetary Rover Simulation', *J Terramech*, 2012, 49, pp. 325-339.
- [21] Weihua Li, Liang Ding, Haibo Gao et al: 'ROSTDyn: Rover simulation based on terramechanics and dynamics', *J Terramech*, 2013, 50, pp. 199-210.
- [22] MC Cavusoglu, D Feygin, F Tendick: 'A Critical Study of the Mechanical and Electrical Properties of the PHANToM Haptic Interface and Improvements for High Performance Control', *Presence: Teleoperators & Virtual Environments*, 2002, 11, (6), pp. 555-568.
- [23] Weihua Li, Zhen Liu, Haibo Gao, Liang Ding, Nan Li and Zongquan Deng: 'Soil Parameter Modification Used for Boosting Predictive Fidelity of Planetary Rover's Slippage', *J. Terramech.*, 2014, 56, pp. 173-184.